Fermi National Accelerator Laboratory

FERMILAB-Conf-87/37-E
7000.691
[CBPF-NF-031/87]

Charm Photoproduction Results from the Fermilab Tagged Photon Spectrometer

J.C. Anjos, J.A. Appel, S.B. Bracker, T.E. Browder, L.M. Cremaldi,
J.R. Elliott, C. Escobar, P. Estabrooks, M.C. Gibney, G.F. Hartner, P.E. Karchin
B.R. Kumar, M.J. Losty, G.J. Luste, P.M. Mantsch, J.F. Martin, S. McHugh, S.R. Menary
R.J. Morrison, T. Nash, U. Nauenberg, P. Ong, J. Pinfold, G. Punkar, M.V. Purohit,
J.R. Raab, A.F.S. Santoro, J.S. Sidhu, K. Sliwa, M.D. Sokoloff, M.H.G. Souza,
W.J. Spalding, M.E. Streetman, A.B. Stundžia, M.S. Witherell

February 1987

*Invited talk presented at the January 1987 Meeting of the DPF, Salt Lake City, Utah, January 1987

Charm Photoproduction Results from the Fermilab Tagged Photon Spectrometer

J. C. Anjos,[3] J. A. Appel,[5] S. B. Bracker,[8] T. E. Browder,[1]
L. M. Cremaldi,[4] J. R. Elliott,[4,a] C. Escobar,[7] P. Estabrooks,[2]
M. C. Gibney,[4] G. F. Hartner,[8] P. E. Karchin,[1,b] B. R. Kumar,[8]
M. J. Losty,[6] G. J. Luste,[8] P. M. Mantsch,[5] J. F. Martin,[8] S. McHugh,[1]
S. R. Menary,[8] R. J. Morrison,[1] T. Nash,[5] U. Nauenberg,[4] P. Ong,[8]
J. Pinfold,[2] G. Punkar,[1] M. V. Purohit,[5] J. R. Raab,[1] A. F. S. Santoro,[3]
J. S. Sidhu,[2] K. Sliwa,[5] M. D. Sokoloff,[5] M. H. G. Souza,[3] W. J. Spalding,[5]
M. E. Streetman,[5] A. B. Stundžia,[8] M. S. Witherell[1]

[1]University of California, Santa Barbara, California, USA
[2]Carleton University, Ottawa, Ontario, Canada
[3]Centro Brasileiro de Pesquisas Físicas, Rio de Janeiro, Brasil
[4]University of Colorado, Boulder, Colorado, USA
[5]Fermi National Accelerator Laboratory,* Batavia, Illinois, USA
[6]National Research Council, Ottawa, Ontario, Canada
[7]Universidad de São Paolo, São Paolo, Brasil
[8]University of Toronto, Toronto, Ontario, Canada

Invited talk presented at the January 1987 meeting of the DPF by
Milind V. Purohit

Abstract

We report results from a preliminary analysis of approximately 30 million reconstructed events (30% of the data) from E-691, a charm photoproduction experiment conducted at the Fermilab Tagged Photon Laboratory in 1985. We present ratios of antiparticles to particles, p_T^2 distributions, x_F distributions, the total charm production cross-section and its energy dependence and the fraction of D^0s from D^*s.

---

[a]Now at Electro Magnetic Applications, Inc., Denver, CO, USA.

[b]Now at Yale University, New Haven, CT, USA.

*Operated by the Universities Research Association, Inc. under contract with the United States Department of Energy.

INTRODUCTION

Until recently, charm hadro- and photo-production experiments have typically reconstructed 10–100 events with a charm decay in any one mode. These numbers severely limit studies of production. E-691, a charm photoproduction experiment conducted at the Fermilab Tagged Photon Lab has reconstructed 30% of its 100 million hadronic events so far, already giving us $\sim$ 3000 fully reconstructed charm decays. In this talk we focus on the production mechanism physics that we have studied using this sample (see also [Anj 86]).

We will begin with a short description of the photon beam and the spectrometer, paying particular attention to the flux, triggers and vertex detector. We then explain the procedure for extracting charm signals. Next we briefly review the current status of hadro- and photo-production of charm experiments along with a general discussion of effects expected from present-day models. Finally, we present results from E-691 and comment on comparisons with models and other experiments.

BEAM AND SPECTROMETER

A 260 GeV electron beam with a momentum bite of 3.4% impinged on a 20% radiation length copper radiator. The resulting bremsstrahlung photons were incident on a 5 cm long Be target. Electrons which radiated photons in the 80-230 GeV range were bent by a magnet and entered a system of shower counters which measured their energy. Scalers counted the number of electrons showering in each individual counter and another scaler counted the total number of showers (at all times as well as when the data acquisition was live). These were used as our main flux monitors. A Monte Carlo reproduces the shape of the photon spectrum well.

Immediately downstream of the target were 9 planes of $50\mu m$ pitch silicon microstrip detectors (SMDs), which improved both tracking efficiency and resolutions. The SMDs were also crucial in reducing the non-charm background (by a factor of $\sim$ 100 to $\sim$ 300 depending on the decay mode) by identifying, event-by-event, a downstream vertex. The transverse resolution of vertices was $\approx$ 20-30μm. For 60 GeV D mesons, the resolution in the beam direction was $\approx$ 300-400μm.

Following the SMDs was a system of 35 drift chamber planes, 2 magnets (M1 and M2), 2 threshold gas Čerenkov counters and electromagnetic and hadronic calorimeters, followed by a steel wall and muon identification scintillation counters. Earlier versions of the SMDs and the downstream detector have been described in detail elsewhere [App 86, Kar 84, Kum 87]. The mass resolutions for the D^0 and D^+ lie between 5 and 10 MeV/c^2. The Čerenkov counters separate pions from kaons in the momentum range 6 – 38 GeV/c.

It is important for studies of the charm production dynamics to have an unbiased trigger while, at the same time, reducing the high trigger rate of non-charmed events. We chose to run with two triggers: a total hadronic trigger which accepted all hadronic events and with which we collected 10% of our data sample and a fast analog global transverse energy trigger. The total hadronic trigger merely required an interaction in the target and at least 40 GeV in the calorimeters. The E_T trigger required a minimum calorimetrically measured E_T in addition; it became 50% efficient at an E_T around 2.5 GeV, keeping $\sim$ 80% of the charm events and only $\sim$ 30% of non-charmed events.

CHARM SIGNALS

While E-691 has obtained clean high-statistics signals in several charm decay modes, we will concentrate here on the three with the highest statistics: $D^0 \to K^-\pi^+$, $D^+ \to K^-\pi^+\pi^+$ and $D^0 \to K^-\pi^+\pi^+\pi^-$. The signals in these three modes are 1370±52, 1118±47 and 432±27 events respectively. In order to reduce the background under the signal in the last mode we require that the D^0 be from the decay of a D^{*+}. Throughout this talk charge-conjugate decays are implied in any discussion. In Table 1 below, we summarize the important cuts applied to events to extract our signals (see also [Anj 87]). Shown in the first column is the effect of each cut in reducing the sample size for the $D^0 \to K^-\pi^+$ mode.

Fraction Accepted in $D^0 \to K^-\pi^+$	$D^0 \to K^-\pi^+$	$D^+ \to K^-\pi^+\pi^+$	$D^0 \to K^-\pi^+\pi^+\pi^-$
$> 1/2$	Geometric Acceptance	Same	Same
$\sim 4/5$	Tracks must traverse SMDs & M1	Same	Same
$< 3/4$	Joint Čerenkov prob. > 0.2	Same	Same Also slow pion prob. > 0.5
$\sim 1/3$	Pri. vtx. $\chi^2/DF < 3.0$	Same	Same
	Sec. vtx. $\chi^2/DF < 3.5$	Same	Same
	Separation $\Delta z/\sigma(\Delta z) > 8.0$	$> 10.$	$> 5.$

Table 1. The charm selection cuts and the fraction by which each cut reduces the remaining signal sample size for the first mode, $D^0 \to K^-\pi^+$.

Figure 1 is a picture of an E-691 charm decay in the vertex region. Seen clearly are the primary vertex and the two secondary vertices from charm decay. While most charm events do not have both secondary vertices reconstructed, the SMDs are very useful in reducing non-charm background for single reconstructed secondary vertices. In the $D^0 \to K^-\pi^+$ mode, for instance, a cut on the vertex separation of $\Delta z/\sigma(\Delta z) > 3$ gives approximately equal amounts of signal to background in the signal region. When the cut is raised to $\Delta z/\sigma(\Delta z) > 12$, the ratio of signal to background is ~6 while the signal has been depleted by only a factor of 2. Figures 2, 3 and 4 are the mass plots for the three decay modes.

CURRENT STATUS OF THEORY AND EXPERIMENT

In the vector meson dominance model (VMD) [Fey 72, Roy 80, Hol 85] photoproduction of open charm is related to production with an incident J/ψ beam. This latter mechanism is unmeasured and there is an additional uncertainty from the Q^2 dependence of the photon-ψ coupling. However, this model does predict that the total cross-section for charm production should reach a constant value when the c.m. energy is

large compared to threshold. In practice this region would be E_γ >100 GeV. The tree-level diagram for photon-gluon fusion (PGF) [Shi 76, Bab 78, Fri 78, Jon 78, Glu 78] describes the production of a $c\bar{c}$ pair, but it does not conserve colour and non-perturbative effects and the hadronization of the quarks are additional unknowns. However this model, unlike VMD, predicts more than the total cross-section: it predicts its energy dependence and the detailed differential cross-section.

There are several reviews of hadroproduction [Rit 84, Mac 86, Lee 86, and Reu 86] and photoproduction [Nas 83 and Hol 85] experiments. From these it is clear that the mean p_T^2 in hadroproduced charm is approximately 1 GeV^2, a result that agrees well with the fusion model if the mean parton k_T^2 is assumed to be ~0.65 GeV^2. When hadroproduction experiments parameterize their x_F distributions with the form

$$\frac{dN}{dx_F} \sim (1 - x_F)^n \qquad (1)$$

they find values of n which vary from 1 to 7. There is some evidence that leading charmed mesons have flatter x_F distributions. Fusion model calculations tend to predict softer distributions which fit the data well below x_F=0.3.

Total cross-sections are hard to compare because it is not obvious how to compare data from different nuclear targets. When cross-sections for hadroproduction of lighter mesons are parameterized as having an A^α dependence, it is known that α has a strong x_F dependence, varying from 0.75 at x_F=0 to 0.45 at x_F=1. Fermilab experiment E-613, a neutrino sensitive beam dump experiment, obtained the value α=0.75±0.05 for charm production [Duf 85]. However, comparisons of LEBC-EHS data with E595 [Rit 84] or ACCMOR [Reu 86] lead to somewhat larger values of α (0.8–1). This problem may be circumvented altogether by comparing experiments using the same nuclear target. In the case of proton targets, LEBC data [Agu 84, Gos 86 and Amm 86] indicate cross-sections of the order of 20μb at $\sqrt{s}$=27 GeV and ~30μb at $\sqrt{s}$=39 GeV with a ratio of $1.7^{+0.6}_{-0.5}$. ISR data indicate a much larger charm production cross-section (several hundred μb) at $\sqrt{s}$=60 GeV based on their observations of Λ_c^+ [Gib 79 and Dri 79]. Fusion model calculations are in good agreement with the energy rise seen by LEBC (although the ratio has large errors),

but there is considerable uncertainty regarding the total cross-section itself. Older calculations [Gos 86] indicate that the observed cross-sections are higher by a factor of ≈2–3 compared to fusion model calculations, while a more recent calculation [Ell 86] indicates that the theoretical uncertainties are larger than believed earlier and may in fact cover the measured cross-sections, except possibly for ISR data.

Prominent among the photoproduction experiments are E-87, the SLAC Hybrid photon experiment, WA58 and a ψ production experiment, E-401. Two major muon experiments, the EMC and BFP, also provide data from virtual photons which can be extrapolated to $Q^2=0$ for comparisons with production from real photons. Important results from these experiments are summarized below:

Experiment	Ref.	Major result
E-87	Hol 85	$< p_T >\sim 1/2$ GeV for D*
SLAC Hybrid	Abe 86	$\sigma_{TOT}=(62\pm8^{+15}_{-10})\times10^{-3}\mu$b at E_γ=20 GeV $\sigma(\overline{D}\Lambda_c^+X)/\sigma_{TOT}=(71\pm11\pm6)\%$
WA58	Ada 86	$\sigma_{TOT}=(0.23\pm.06)\mu$b (assuming A^1 dependence) at 20 GeV < E_γ < 70 GeV $\sigma(\overline{D}\Lambda_c^+X)/\sigma_{TOT}=(28\pm23)\%$ $\sigma(\overline{D}DX)/\sigma_{TOT}=(70\pm21)\%$
E-401	Hol 85	$\gamma N \rightarrow \psi N$ (elastic) σ(200 GeV)/σ(100 GeV)=1.56±0.20 (statistical errors only)
EMC	Aub 83	$\mu\mu$ and $\mu\mu\mu$ events from virtual photons. Good agreement with PGF for Q^2, ν, p_T and $\Delta\phi$ distributions without correction for overall normalization using $xG(x)=3(1-x)^5$ σ(200 GeV)/σ(100 GeV)=1.53±0.20 (statistical errors only)
BFP	Cla 80	Comments as for EMC σ(200 GeV)/σ(100 GeV)=1.44±0.20 (statistical errors only)

Table 2. Results from major photoproduction experiments.

As we can see, there are three experiments with data on the rise of the total charm cross-section, if we assume that the E-401 result holds for open charm production. There is no good information on the p_T^2 and x_F distributions of charmed mesons, or the total cross-section. There is no information on the A-dependence of open charm production, although the A-dependence of J/ψ production has been measured [Sok 86] as α=0.94±.02±.03 for incoherent production. It would appear that associated production decreases dramatically from 20 GeV (SLAC experiment) to the somewhat higher energy range (20-70 GeV) of WA58. Whether this trend continues is a very interesting question as it throws light on how the $c\bar{c}$ pair is hadronized. Hadronization when the quark couples to a diquark in the target nucleus would favour lower values of x_F for particles as opposed to antiparticles.

E-691 RESULTS

We have obtained background subtracted and acceptance corrected p_T^2 and x_F distributions for the three modes described earlier. In Figures 5 and 6 we show these distributions for the $D^0 \rightarrow K^-\pi^+$ mode, the other distributions being similar. We fit the p_T^2 distribution to the form $dN/dp_T^2 \sim \exp(-ap_T^2)$ and the x_F distribution to the form (1). Notice that we have cut off the x_F distribution below x_F=0.2, thereby limiting ourselves to a region where the detector acceptance is well understood. We have investigated the systematic effects arising from the bias due to the E_T trigger, due to smearing of kinematic quantities, due to Fermi motion [Bod 81], due to vertexing and other cuts and due to uncertainty in the acceptance correction calculation. For the x_F distributions, we have also investigated the effects due to the ~8% smearing of the photon energy by the tagging system. For these studies we have used a Monte Carlo based on the PGF model followed by the Lund Monte Carlo for hadronization [Sjö 85]. The Monte Carlo gives a good representation of the detector and associated multiplicities. The table below summarizes our results. The systematic errors on the ratio of antiparticles to particles are small compared to the present statistical errors. It is interesting to note that the Monte Carlo, with its present default parameters (yet to be varied for a detailed study), yields a $< p_T^2 >$=1.35 GeV^2 and 2.5 for the power of $(1-x_F)$ in the x_F distribution.

Mode	Number of $\overline{D}/D$	$< p_T^2 >$ (GeV^2)	n, where $d\sigma/dx_F \sim (1-x_F)^n$ $x_F > 0.2$
$D^0 \to K^-\pi^+$	0.99±.07	1.37±.06±.08	2.7±.2±.4
$D^+ \to K^-\pi^+\pi^+$	1.03±.07	1.29±.09±.08	2.6±.2±.4
$D^0 \to K^-\pi^+\pi^+\pi^-$	1.07±.12	1.34±.13±.08	2.8±.3±.6
Combined	1.02±.05	1.34±.05±.08	2.7±.1±.6

Table 3. Summary of E-691 results for the ratio of antiparticles to particles, $< p_T^2 >$, and x_F distributions.

While the entire sample of $D^0 \to K^-\pi^+\pi^+\pi^-$ candidates comes from D^{*+} decays, we have examined the $D^0 \to K^-\pi^+$ sample to determine that (31.3±2.4)% of the D^0s arise from D^{*+} decays (after correcting for acceptance). This is consistent with the expectation of (27±3)% of D^0s being from this source if one assumes a 3:1 production ratio for D*s to Ds and the 1986 PDG branching ratios [PDG 86].

The total charm production cross-section has been measured in the region $x_F > 0.2$. In order to check our flux measurement, we have determined the total hadronic cross-section *per nucleus* on Be to be (824±78) μb, consistent with the expected value of (861±40) μb [Mor 86]. Using our Monte Carlo for acceptance corrections, and the data for trigger efficiencies, we determine the total cross-section for D^0s and D^+s to be 1.70±.16 μb and 0.81±.09 μb *per Be nucleus* in the range $x_F > 0.2$ with statistical and some of the systematic errors only. Extrapolating to all x_F involves dependence on theoretical models; so does the conversion to $c\bar{c}$ production (because of events containing both a D^0 and a D^- and the missing cross-section from D_s^+, Λ_c^+ etc. production). We have made these extrapolations using the Monte Carlo described earlier to get

$$\sigma_{TOT}(c\bar{c}) = (3.17 \pm .22 \pm .8)\mu\text{b on Be nuclei.}$$

at our energies (≈170 GeV). While it is not known what the A-dependence should be, it is reasonable that α lies between 2/3 and 1. This leads to a difference of a factor of two when the *per Be* cross-section is extrapolated to a *per nucleon* cross-section!

Finally, we have studied the rise of the total charm production cross-section with energy. Figure 7 shows the uncorrected energy distribution of charm events, to be contrasted with the falling bremsstrahlung photon spectrum. The detector acceptance does not change appreciably with energy, but is an important effect that we correct. The resulting rise is fit to a linear increase with energy (Figure 8). The ratio of the cross-section at 200 GeV to that at 100 GeV was determined by combining the three decay modes weighted by their relative production cross-sections. We obtain

$$\frac{\sigma(E_\gamma = 200GeV)}{\sigma(E_\gamma = 100GeV)} = 1.83 \pm .29 \pm .37$$

This rise is consistent with the three values from other experiments quoted in Table 2. Calculations using the PGF model show a strong dependence on the power of (1-x) in the gluon structure function, going from 1.6 with n=5 to 2.0 with n=9 and a scaling distribution. There is a milder dependence on the assumptions about m_c (the mass of the charmed quark) and the QCD constant Λ.

CONCLUSIONS

A preliminary analysis of 30% of the data sample from E-691 has yielded information about the photoproduction of charm, including x_F distibutions and the ratio of D*s to Ds. The $< p_T^2 >$ of D mesons is determined to be $1.34 \pm .05 \pm .08$ GeV^2. In our (mostly forward) acceptance region, we find that the ratio of antiparticles to particles is $1.02 \pm .05$. This indicates that there is very little associated production at our energies. The total cross-section for charm production is $(3.17 \pm .22 \pm .8)\mu$b *per Be nucleus*, with model dependent assumptions. The ratio of cross-sections at 200 GeV and 100 GeV is determined to be $1.83 \pm .29 \pm .37$, consistent with previous experiments and the PGF model. We expect to continue studies of photoproduction of charm, concentrating in particular on improving our understanding of the detector acceptance and extracting the gluon structure function from the sample of events where both charmed particles are fully reconstructed.

ACKNOWLEDGEMENTS

We gratefully acknowledge the assistance of the staff of Fermilab

and of all the participating institutions. This research was supported by the U. S. Department of Energy, by the Natural Science and Engineering Research Council of Canada through the Institute of Particle Physics, by the National Research Council of Canada and by the Brazilian Conselho Nacional de Desenvolvimento Científico e Tecnológico.

REFERENCES

Abe 86 Abe, K. et al., Phys. Rev. D33, 1 (1986).

Ada 86 Adamovich, M. I. et al., CERN/EP 86-89 (1986).

Agu 84 Aguilar-Benitez, M. et al., Phys. Lett. 135 237, (1984).

Amm 86 Ammar, R. et al., LEBC-MPS collaboration, CERN/EP 86-122, 1986.

Anj 86 Anjos, J. C. et al., in the "Proceedings of the XXIII International Conference on High Energy Physics", Berkeley, CA, 1986.

Anj 87 Anjos, J. C. et al., Phys. Rev. Lett., 58, 311 (1987).

App 86 Appel, J. A. et al., Nucl. Instr. and Meth., A243, 361 (1986) and references therein.

Aub 83 Aubert, J. J. et al., Nucl. Phys. B213, 31 (1983).

Bab 78 Babcock, J., Sivers, D. and Wolfram, S., Phys. Rev. D18, 162 (1978).

Bod 81 Bodek, A. and Ritchie, J. L., Phys. Rev. D23, 1070 (1981).

Cla 80 Clark, A. R. et al., Phys. Rev. Lett. 45, 682 (1980).

Duf 85 Duffy, M. E. et al., Phys. Rev. Lett. 55, 1816 (1985).

Ell 86 Ellis, R. K. in the "Proceedings of the XXI Rencontre de Moriond," 1986. (Fermilab-Conf-86/35-T).

Fey 72 Feynman, R. P., Photon Hadron Interactions. Reading, Mass: Benjamin (1972).

Fri 78 Fritsch, H. and Streng, K. H., Phys. Lett. 72B, 385 (1978).

Glu 78 Gluck, M. and Reya, E. Phys. Lett. 79B, 453 (1978).

Gos 86 Goshaw, A. T., in the Proceedings of the XVII International Symposium on Multiparticle Dynamics, Seewinkel, Austria, 1986.

Hol 85 Holmes, S. D., Lee, W. Y. and Wiss, J. E., Ann. Rev. Nucl. Part. Sci., 35, 397 (1985).

Jon 78 Jones, L. M. and Wyld, H. W., Phys. Rev. D17, 759 (1978).

Kar 84 Karchin, P., et al., IEEE Trans. on Nucl. Sci. NS-32, 612 (1985).

Kum 87 Kumar, B. R. in the Proceedings of the Workshop on Vertex Detectors, Erice, Italy, 1986. Published by Plenum Press, 1987.

Lee 86 Leedom, I. D., Fermilab TM-1396 (1986).

Mac 86 MacDermott, M., in the Proceedings of the Twentieth Rencontre de Moriond (1985), edited by J. Tran Tranh Van.

Mor 86 Morrison, R. J., private communication. The number comes from data on cross-sections measured in various experiments performed by Morrison et al. on targets other than Be, but the A-dependence is very accurately known.

Nas 83 Nash, T. in *Proceedings of the International Symposium on Lepton and Photon Interactions at High Energies, Ithaca, New York, 1983*, ed. D. Cassel et al., Cornell University, Ithaca, 1983.

PDG 86 Particle Data Group, Phys. Lett., 170B, 1 (1986).

Reu 86 Reucroft, S., VI International Conference on Physics in Collision, Chicago (1986).

Rit 84 Ritchie, J. L., in the Proceedings of the Snowmass workshop, 1984.

Roy 80 Roy, D. P., Phys. Lett. 96B, 189 (1980).

Shi 76 Shifman, M. A., Vainstein, A. I. and Zakharov, V. I., Phys. Lett. 65B, 255 (1976).

Sjö 85 Sjöstrand, T., LU TP 85-10, University of Lund, Sweden.

Sok 86 Sokoloff, M. D. et al., Phys. Rev. Lett., 57, 3003 (1986).

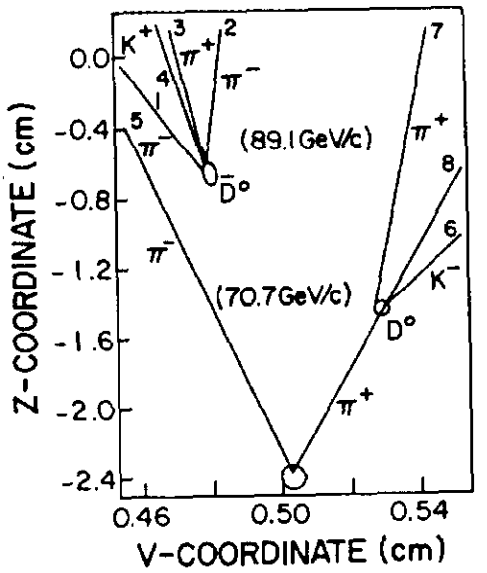

Figure 1. An E-691 charm event: magnified view of the vertex.

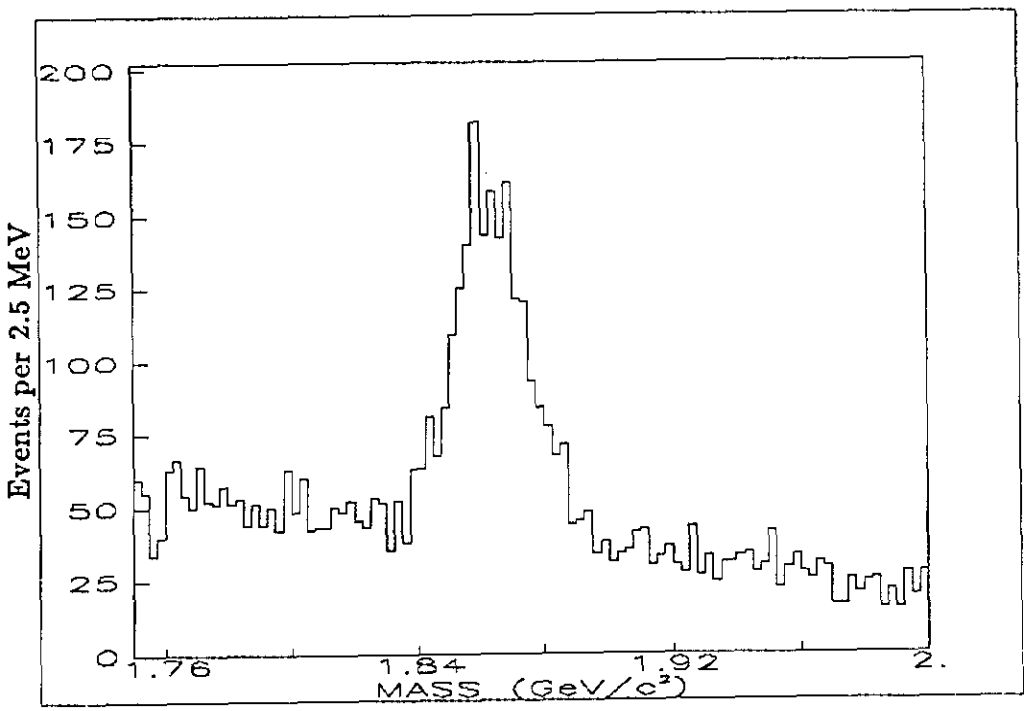

Figure 2. The $D^0 \rightarrow K^-\pi^+$ mass plot.

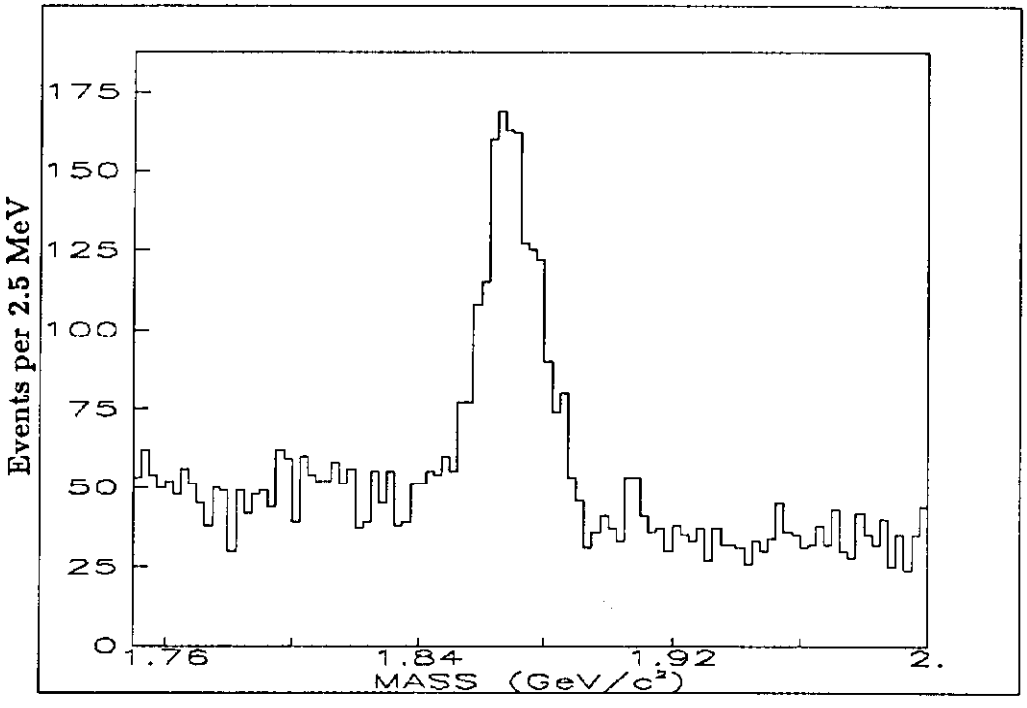

Figure 3. The $D^+ \to K^-\pi^+\pi^+$ mass plot.

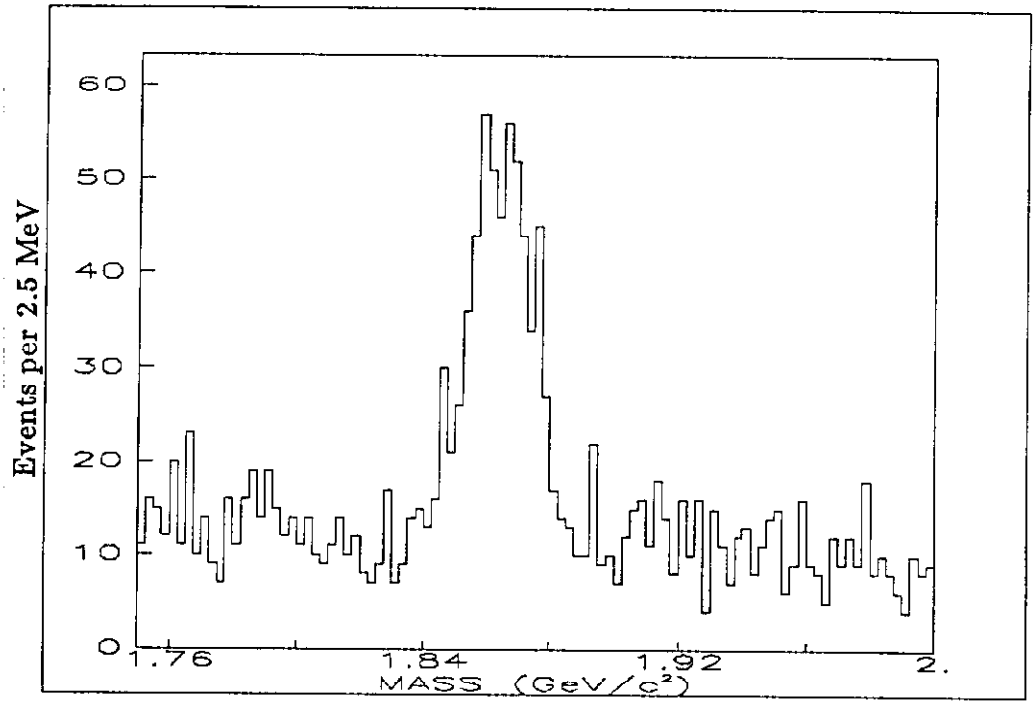

Figure 4. The $D^0 \to K^-\pi^+\pi^+\pi^-$ mass plot.

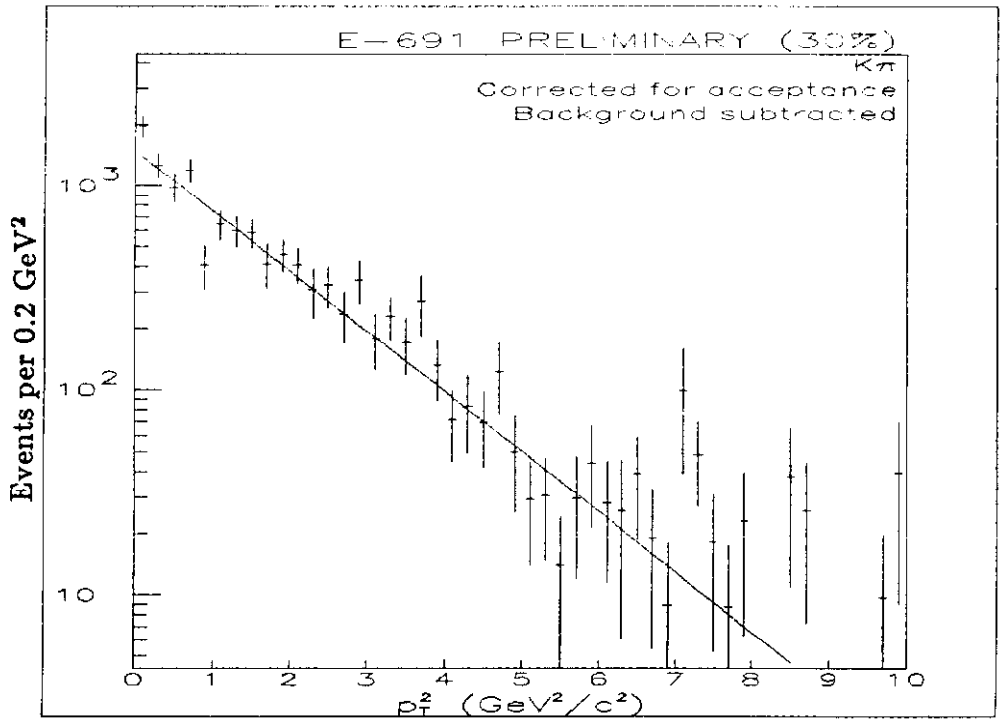

Figure 5. The p_T^2 distribution for the $D^0 \to K^-\pi^+$ mode. The solid line is the fit described in the text.

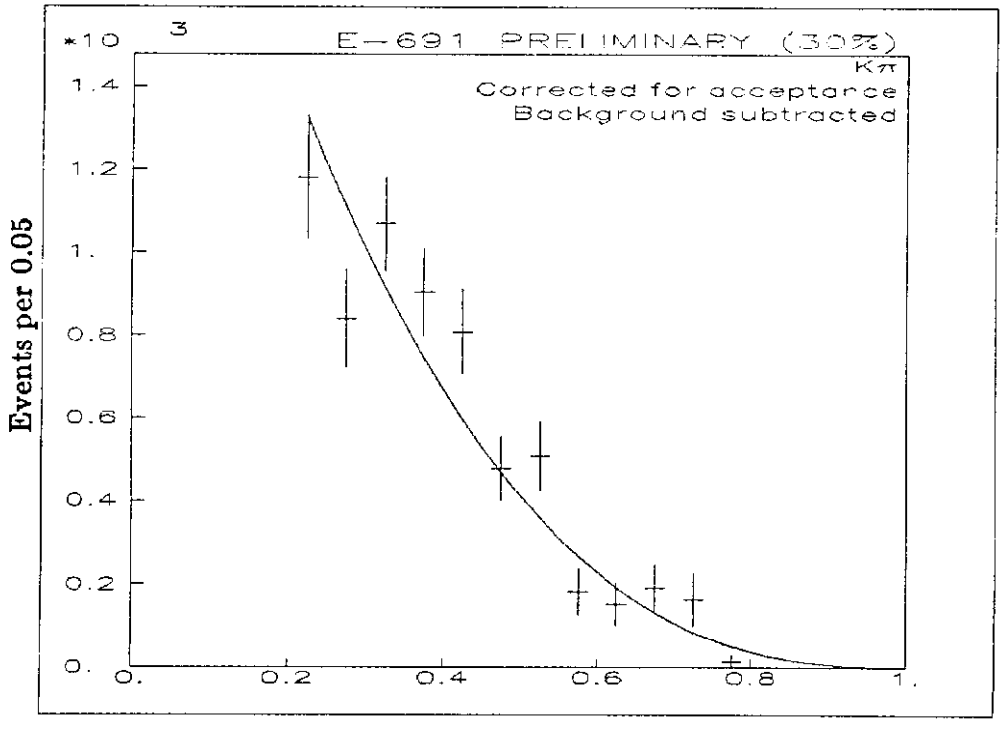

Figure 6. The x_F distribution for the $D^0 \to K^-\pi^+$ mode for $x_F > 0.2$. The solid line is the fit described in the text.

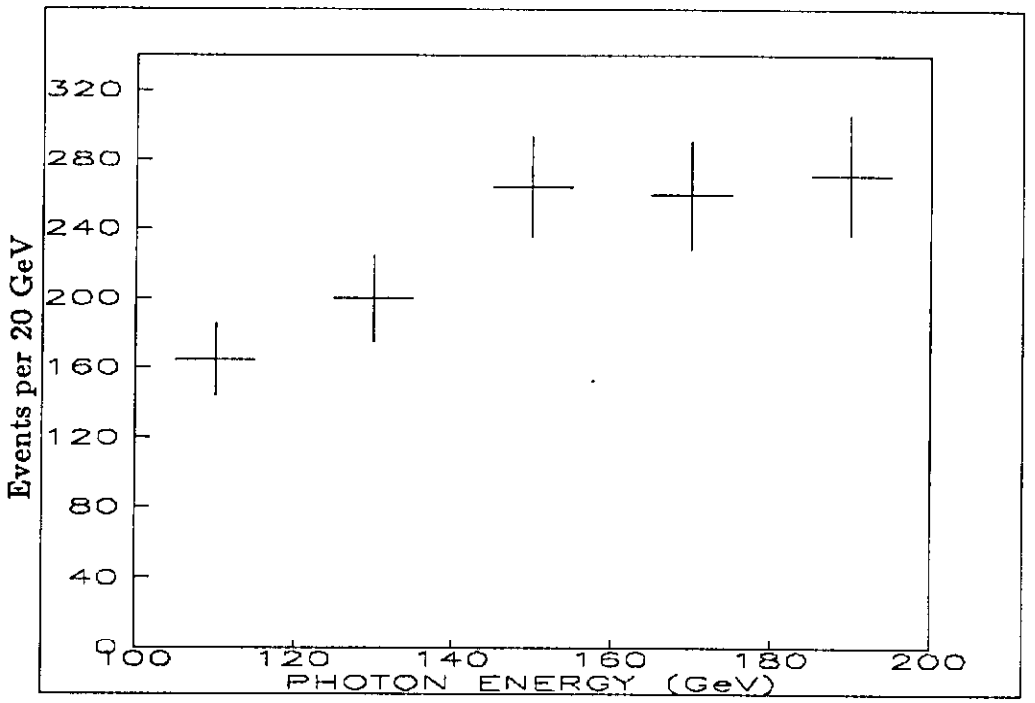

Figure 7. The background subtracted energy distribution of charm events (not corrected for acceptance).

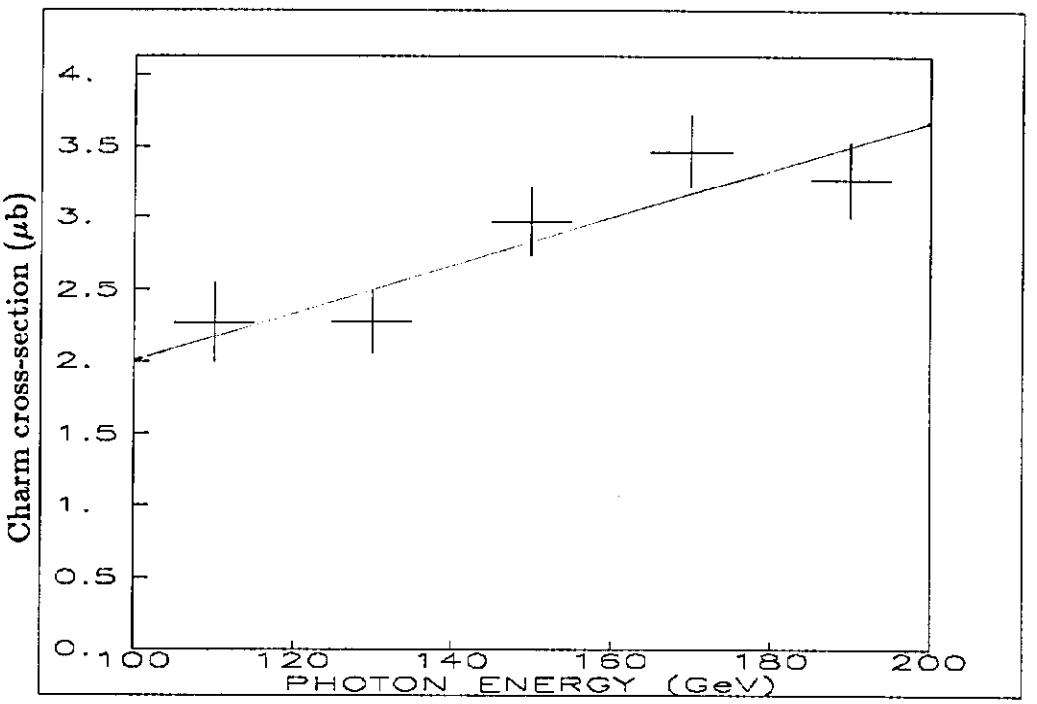

Figure 8. The rise of the total charm cross-section with energy. The solid line is the fit described in the text.